# Quantum Mechanical Hydrogen Exchange Coupling in $[(C_5H_5)Ir(L)H_3]^+$ Complexes (L = $PH_3$, CO). A Combined ab Initio/Tunneling Dynamics Study

**Abdellah Jarid,[‡] Miquel Moreno, Agustí Lledós,* José M. Lluch,* and Juan Bertrán**

*Contribution from the Departament de Química, Universitat Autònoma de Barcelona, 08193 Bellaterra, Barcelona, Spain*

*Received March 31, 1994*[®]

**Abstract:** Quantum mechanical hydrogen exchange coupling in $[(C_5H_5)Ir(L)H_3]^+$ complexes (L = $PH_3$, CO) has been studied by combining the construction of *ab initio* potential energy surfaces with a tunneling model using a basis set method. Our results show that these transition-metal trihydride complexes may exchange a pair of hydrogens through a tunneling path which involves a transition state with a $\eta^2$-$H_2$ structure. The energy barriers for L = $PH_3$ and CO are respectively 14.1 and 10.7 kcal/mol, leading to exchange coupling constants of 112.3 and 1279.5 Hz, respectively. These values are in satisfactory agreement with experimental results. Temperature dependence of the exchange couplings is also analyzed and shown to be in accordance with experiments. Finally, the effect of the substitution of one or both of the exchanging hydrogens by deuterium is considered.

## I. Introduction

The proton NMR spectra of several transition-metal trihydride complexes $L_nMH_3$ have recently attracted considerable interest.[1−4] The three hydride protons exhibit the expected $AB_2$ pattern, but the apparent $J_{AB}$ values show a large temperature dependence and striking isotope effects. The large $J_{AB}$ values for $[(C_5H_5)Ir(L)H_3]^+$ (L = various phosphine and phosphite ligands) ranging from 61 to 1565 Hz are well outside the normal range of H−H coupling constants.[1b]

The physical phenomenon behind these big $J_{AB}$ values has been recognized as due to quantum mechanical exchange of a pair of identical $H_1$ and $H_2$ hydrides between two chemically inequivalent A and B sites.[5] Thus, two possible situations can be envisaged: $H_1$ and $H_2$ are at sites A and B, respectively, or conversely, $H_2$ and $H_1$ lie at sites A and B, respectively, an exchange between the pair of hydrogens having been produced. Note that, in spite of A and B sites being inequivalent, both situations are energetically degenerate because $H_1$ and $H_2$ are identical particles.

**Scheme 1**

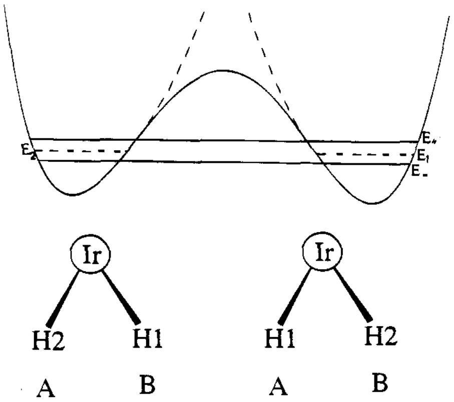

These two equivalent configurations can be associated with two wells separated by an energy barrier in such a way that the exchange process can be analyzed by means of a double well model (see Scheme 1).

If the barrier were infinite there would be two uncoupled stationary states $\psi_1$ and $\psi_2$, located in each side of the double well with energies $E_1 = E_2$. In this case there would be no tunneling connecting both wells.

When the barrier is finite, a coupling $J$ takes place between both wells so that $\psi_1$ and $\psi_2$ are no longer stationary states of the system. It can be easily demonstrated[6] that the new stationary states $\psi_+$ and $\psi_-$ have associated energies $E_+$ and $E_-$ so that an energy splitting appears: $E_+ - E_- = -2J$. Since $J$ is intrinsically a negative magnitude, the so-called exchange

---

[‡] Permanent Address: Département de Chimie, Faculté des Sciences, Université Moulay Ismaïl, Meknès, Maroc.

[®] Abstract published in *Advance ACS Abstracts,* January 1, 1995.

(1) (a) Heinekey, D. M.; Payne, N. G.; Schulte, G. K. *J. Am. Chem. Soc.* **1988**, *110*, 2303. (b) Heinekey, D. M.; Millar, J. M.; Koetzle, T. F.; Payne, N. G.; Zilm, K. W. *J. Am. Chem. Soc.* **1990**, *112*, 909. (c) Heinekey, D. M.; Payne, N. G.; Sofield, C. D. *Organometallics* **1990**, *9*, 2643. (d) Heinekey, D. M.; Harper, T. G. P. *Organometallics* **1991**, *10*, 2891. (e) Heinekey, D. M. *J. Am. Chem. Soc.* **1991**, *113*, 6074.

(2) (a) Arliguie, T.; Chaudret, B.; Devillers, J.; Poilblanc, R. *C.R. Hebd. Séances Acad. Sci. Ser. 2* **1987**, *305*, 1523. (b) Antiñolo, A.; Chaudret, B.; Commenges, G.; Fajardo, M.; Jalon, F.; Morris, R. H.; Otero, A.; Schweltzer, C. *J. Chem. Soc., Chem. Commun.* **1988**, 1210. (c) Chaudret, B.; Commenges, G.; Jalon, F.; Otero, A. *J. Chem. Soc., Chem. Commun.* **1989**, 210. (d) Arliguie, T.; Border, C.; Chaudret, B.; Devillers, J.; Poilblanc, R. *Organometallics* **1989**, *8*, 1308. (e) Arliguie, T.; Chaudret, B.; Jalon, F.; Otero, A.; Lopez, J. A.; Lahoz, F. J. *Organometallics* **1991**, *10*, 1888. (f) Antiñolo, A.; Carrillo, F.; Fernández-Baeza, J.; Otero, A.; Fajardo, M.; Chaudret, B. *Inorg. Chem.* **1992**, *31*, 5156. (g) Antiñolo, A.; Carrillo, F.; Chaudret, B.; Fajardo, M.; Fernández-Baeza, J.; Lanfranchi, M.; Limbach, H.-H.; Maurer, M.; Otero, A.; Pellinghelli, M. A. *Inorg. Chem.* **1994**, *33*, 5163.

(3) Paciello, R. A.; Manriquez, J. M.; Bercaw, J. E. *Organometallics* **1990**, *9*, 260.

(4) The problem has been recently treated in three reviews: (a) Jessop, P. G.; Morris, R. H. *Coord. Chem. Rev.* **1992**, *121*, 155. (b) Heinekey, D. M.; Oldham, W. J., Jr. *Chem. Rev.* **1993**, 913. (c) Crabtree, R. H. *Angew. Chem., Int. Ed. Engl.* **1993**, *32*, 789.

(5) (a) Jones, D. H.; Labinger, J. A.; Weitekamp, D. P. *J. Am. Chem. Soc.* **1989**, *111*, 3087. (b) Zilm, K. W.; Heinekey, D. M.; Millar, J. M.; Payne, N. G.; Demou, P. *J. Am. Chem. Soc.* **1989**, *111*, 3088. (c) Zilm, K. W.; Heinekey, D. M.; Millar, J. M.; Payne, N. G.; Neshyba, S. P.; Duchamp, J. C.; Szczyrba, J. *J. Am. Chem. Soc.* **1990**, *112*, 920. (d) Zilm, K. W.; Millar, J. W. *Adv. Magn. Reson.* **1990**, *15*, 163.

(6) (a) Cohen-Tannoudji, C.; Diu, B.; Laloë, F. *Quantum Mechanics*; John Wiley and Sons: Paris, 1977. (b) Bell, R. P. *The Tunnel Effect in Chemistry*; Chapman and Hall: London, 1980.

0002-7863/95/1517-1069$09.00/0

coupling $-2J$ is positive. If a magnetic scalar coupling $J_m$ is also present, then the total observed coupling is $J_T = J_m - 2J$.

Heinekey *et al.*[5b,c] have estimated the value of the coupling constant in the above-mentioned series of iridium complexes by using a set of parameters suitable for a pair of protons in Landesman's model.[7] This model is a crude approximation based on a hard spheres potential. Barthelat *et al.*[8] have used the same formula, taking the parameters from *ab initio* calculations on [$Cp_2MH_3$] complexes with M = niobium and tantalum to show that the niobium complex presents high couplings, whereas they are absent in the isostructural and isoelectronic tantalum complex.

The purpose of this paper, as a continuation of a previous letter,[9] is to provide a theoretical calculation of these exchange couplings from first principles. To this aim we have combined the construction of an *ab initio* potential energy surface with a realistic tunneling model. We have chosen complexes of the type $[(C_5H_5)Ir(L)H_3]^+$ for which extensive experimental data have been previously obtained by Heinekey *et al.*[1b,5c] Specifically, $[(C_5H_5)Ir(PH_3)H_3]^+$ and $[(C_5H_5)Ir(CO)H_3]^+$ complexes have been studied. Comparison between the results corresponding to both transition-metal trihydrides enables us to discuss the sensitivity of the exchange couplings to ligand substitution. Their temperature dependence and the primary isotope effects are also explained by this model.

## II. Methodological Details

In what follows, we will begin in subsection A by describing the *ab initio* calculations that will be employed to build up the potential energy surface, and then, in subsection B, we will present the tunneling model used in this paper.

**A. Ab Initio Calculations.** *Ab initio* self-consistent field (SCF) calculations have been carried out with the GAUSSIAN 92 series of programs.[10] The basis set used was of valence triple-$\zeta$ quality for the iridium atom,[11a] valence double-$\zeta$ for phosphorus,[11b] carbons,[11c] oxygens,[11c] and hydrogens[11c] of the $C_5H_5$, $PH_3$, and CO groups, and double-$\zeta$ + polarization functions for the three hydrides.[11c,d] An effective core potential operator has been used for the core electrons of iridium[11a] and phosphorus atoms.[11b] In some cases, which will be commented on below, correlation energy was introduced by using the Møller–Plesset perturbation theory up to second order (MP2),[12] which recently has been shown to correctly reproduce the relative stability of classical structures having terminal hydride ligands and nonclassical polyhydride complexes containing $\eta^2$-$H_2$ ligands.[13]

**B. Tunneling Model.** Once the reaction path on the potential energy surface is determined, the quantum exchange will be treated in terms of a one-dimensional tunneling model. As a matter of fact, the exact treatment involving the full configurational space would require a large number of dimensions. However, we think that the present work is a useful computational entry to this problem.

**Table 1.** Geometric Parameters for the $[(C_5H_5)Ir(PH_3)H_3]^+$ Minimum Structure[a]

| | SCF | MP2 | expl[b] |
|---|---|---|---|
| $Ir-H_1$ | 1.581 | 1.598 | 1.591 |
| $Ir-H_2$ | 1.585 | 1.596 | 1.583 |
| $Ir-H_3$ | 1.585 | 1.596 | 1.588 |
| Ir–P | 2.422 | 2.389 | 2.273 |
| Ir–C | 2.373 | 2.385 | 2.238 |
| C–C | 1.431 | 1.458 | 1.412 |
| $H_1\cdots H_2$ | 1.574 | 1.690 | 1.700 |
| $H_1\cdots H_3$ | 1.574 | 1.690 | 1.670 |
| $H_2\cdots H_3$ | 2.602 | 2.726 | 2.660 |
| $\angle H_1-Ir-H_2$ | 59.6 | 64.0 | 64.7 |
| $\angle H_1-Ir-H_3$ | 59.6 | 64.0 | 63.6 |
| $\angle H_2-Ir-H_3$ | 110.4 | 117.1 | 114.4 |
| $\angle H_1-Ir-P$ | 103.4 | 104.6 | 98.3 |
| $\angle H_2-Ir-P$ | 81.9 | 80.6 | 74.7 |
| $\angle H_3-Ir-P$ | 81.9 | 80.6 | 75.8 |

[a] Distances are given in Å and angles in deg. [b] Neutron diffraction values for the $[(C_5H_5)Ir(PMe_3)H_3]^+$ complex.

Symmetric double wells have been built by means of cubic spline functions fitted in such a way that the energy barrier and the path length coincide with the estimated values obtained through *ab initio* calculations, as discussed below.[14] Because we are interested in the evaluation of the exchange coupling, we must obtain the vibrational states of the double well. For this purpose we have used a basis set methodology by taking a set of localized Gaussian functions which have the form[15]

$$\chi_i(s) = \left(\frac{\alpha}{\pi}\right)^{1/4} \exp\left[\frac{-\alpha}{2}(s - s_i)^2\right]$$

where $\alpha$ is an optimizable parameter and $s_i$ values are equally spaced points along the coordinate space. Then, a variational calculation by using $n$ functions provides the lowest $n$ eigenvalues and eigenfunctions of the one-dimensional system. In particular, we have used 81 Gaussian functions throughout all the calculations. We have observed that further increase in the number of basis functions does not appreciably modify the energies of the levels below the barrier.

## III. Hydrogen Exchange in the $[(C_5H_5)Ir(PH_3)H_3]^+$ Complex

The geometry of the $[(C_5H_5)Ir(PMe_3)H_3]^+$ complex has been determined experimentally by neutron diffraction and it clearly shows a trihydride structure.[1b] Table 1 compares this experimental geometry (third column) with the fully optimized geometry of our $[(C_5H_5)Ir(PH_3)H_3]^+$ complex at the Hartree–Fock SCF level (first column). It is clear that our theoretical results are in good agreement with experimental results.

In order to discuss the mechanism by which the exchange of a pair of hydrides occurs, we have built a tridimensional potential energy surface for the $[(C_5H_5)Ir(PH_3)H_3]^+$ complex by taking as grid parameters the distance ($R_{HH}$) between the two hydrogens that are interchanged, $H_1$ and $H_2$, the distance ($R_{MX}$) between the Ir and the midpoint (X) of the $H_1-H_2$ segment, and the rotational angle ($\theta$) of the $H_1-H_2$ bond in the plane orthogonal to the MX direction (see Scheme 2). The remaining geometrical parameters were fixed at the SCF fully optimized values. Using such a geometrical definition, the SCF minimum energy structure corresponds to $R_{HH} = 1.57$ Å, $R_{MX} = 1.37$ Å, and $\theta = 0°$. About 400 SCF energy calculations were performed in order to build up this tridimensional surface. The energies of more than 50 points belonging to the most significant regions of the potential energy surface were recalculated in order to introduce correlation energy, so that all the

---

(7) Landesmann, A. *Ann. Phys. (Fr.)* **1973**, *8*, 53.

(8) Barthelat, J. C.; Chaudret, B.; Daudey, J. P.; DeLoth, P.; Poilblanc, R. *J. Am. Chem. Soc.* **1991**, *113*, 9896.

(9) Jarid, A.; Moreno, M.; Lledós, A.; Lluch, J. M.; Bertrán, J. *J. Am. Chem. Soc.* **1993**, *115*, 5861.

(10) Frisch, M. J.; Trucks, G. W.; Head-Gordon, M.; Gill, P. M. W.; Wong, M. W.; Foresman, J. B.; Johnson, B. G.; Schlegel, H. B.; Robb, M. A.; Replogle, E. S.; Gomperts, R.; Andrés, J. L.; Raghavachari, K.; Binkley, J. S.; González, C.; Martin, R. L.; Fox, D. J.; Defrees, D. J.; Baker, J.; Stewart, J. J. P.; Pople, J. A. *Gaussian 92*; Gaussian Inc.: Pittsburg, PA, 1992.

(11) (a) Hay, P. J.; Wadt, W. R. *J. Chem. Phys.* **1985**, *82*, 270. (b) Wadt, W. R.; Hay, P. J. *J. Chem. Phys.* **1985**, *82*, 284. (c) Binkley, J. S.; Pople, J. A.; Hehre, W. *J. Am. Chem. Soc.* **1980**, *102*, 939. (d) Hariharan, P. C.; Pople, J. A. *Theor. Chim. Acta* **1973**, *28*, 213.

(12) (a) Møller, C.; Plesset, M. S. *Phys. Rev.* **1936**, *46*, 618. (b) Pople, J. A.; Binkley, J. S.; Seeger, R. *Int. J. Quantum Chem.* **1976**, *S10*, 1.

(13) (a) Lin, Z.; Hall, M. B. *Inorg. Chem.* **1991**, *30*, 2569. (b) Lin, Z.; Hall, M. B. *J. Am. Chem. Soc.* **1992**, *114*, 2928. (c) Maseras, F.; Koga, N.; Morokuma, K. *J. Am. Chem. Soc.* **1993**, *115*, 8313. (d) Maseras, F.; Li, X-K.; Koga, N.; Morokuma, K. *J. Am. Chem. Soc.* **1993**, *115*, 10974.

(14) Bosch, E.; Moreno, M.; Lluch, J. M.; Bertrán, J. *J. Chem. Phys.* **1990**, *93*, 5685.

(15) (a) Hamilton, I. P.; Light, J. *J. Chem. Phys.* **1986**, *84*, 306. (b) Makri, N.; Miller, W. H. *J. Chem. Phys.* **1987**, *86*, 1451.

**Scheme 2**

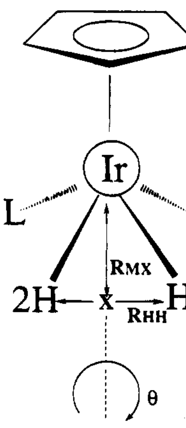

energy values reported hereafter in this paper will correspond to the MP2 level.

To visualize the main features of the MP2 tridimensional surface, in Figure 1 we have depicted two bidimensional potential energy surfaces extracted from the data contained in the MP2 tridimensional surface. In the first bidimensional surface (Figure 1a), the reduction of the dimensionality is accomplished by optimizing in the 3-D surface the $R_{HH}$ distance for each pair of $R_{MX}$ and $\theta$ parameters. Then, the energy is plotted as a function of these two parameters ($R_{MX}$ and $\theta$). On the other hand, Figure 1b is a cut of the tridimensional surface, and it presents the energy as a function of $R_{HH}$ and $R_{MX}$ parameters, by keeping the $\theta$ angle frozen at its initial zero value. In Figures 1a and 1b several relevant points can be identified. Point **1**, at $\theta = 0°$ and $R_{MX} = 1.37$ Å (with $R_{HH} = 1.57$ Å), has the geometry corresponding to the minimum energy structure above located at the SCF level. Point **3** is a transition state, which appears at $\theta = 90°$ and $R_{MX} = 1.72$ Å (with an $R_{HH}$ optimized value of 0.88 Å), and it has a geometry corresponding to a 90° rotated $\eta^2$-$H_2$ entity, imposing an energy barrier of 14.4 kcal/mol with respect to point **1**.

The SCF minimum energy structure and the transition state located in our reduced three-dimensional surface, however, do not necessarily correspond to the same points in the full-dimensional MP2 energy hypersurface. In order to test the validity of our methodology, we have evaluated the minimum energy structure by a complete optimization in the full potential energy surface at the MP2 level (only the cyclopentadienyl group has been forced to keep the planarity). The transition state has also been located as a stationary point with only one negative eigenvalue of the second derivative matrix force.

The MP2 geometry of the minimum is presented in the second column of Table 1 where it is compared with the SCF results and the experimental values.[1b] The transition state geometry is presented in Table 2.

Results in Table 1 clearly show that MP2 and SCF geometries are very similar, both showing good agreement with experimental results. In the transition state, comparison of geometries also shows only slight differences in geometry: the parameters that were kept frozen in the reduced 3-D optimization are not appreciably modified by the optimization. As for the most important geometrical parameters that involve the exchanging hydrogen coordinates, they show very similar values in both cases. For instance, $R_{HH}$ is 0.892 Å for the "true" transition state, whereas for the point located in the 3-D surface the value is 0.88 Å. This similarity is reflected in the very close energies of both structures so that the energy barrier changes only from 14.4 to 14.1 kcal/mol. Therefore, comparison of geometries and energies confirms the validity of the strategy used to build up the reduced 3-D energy surface.

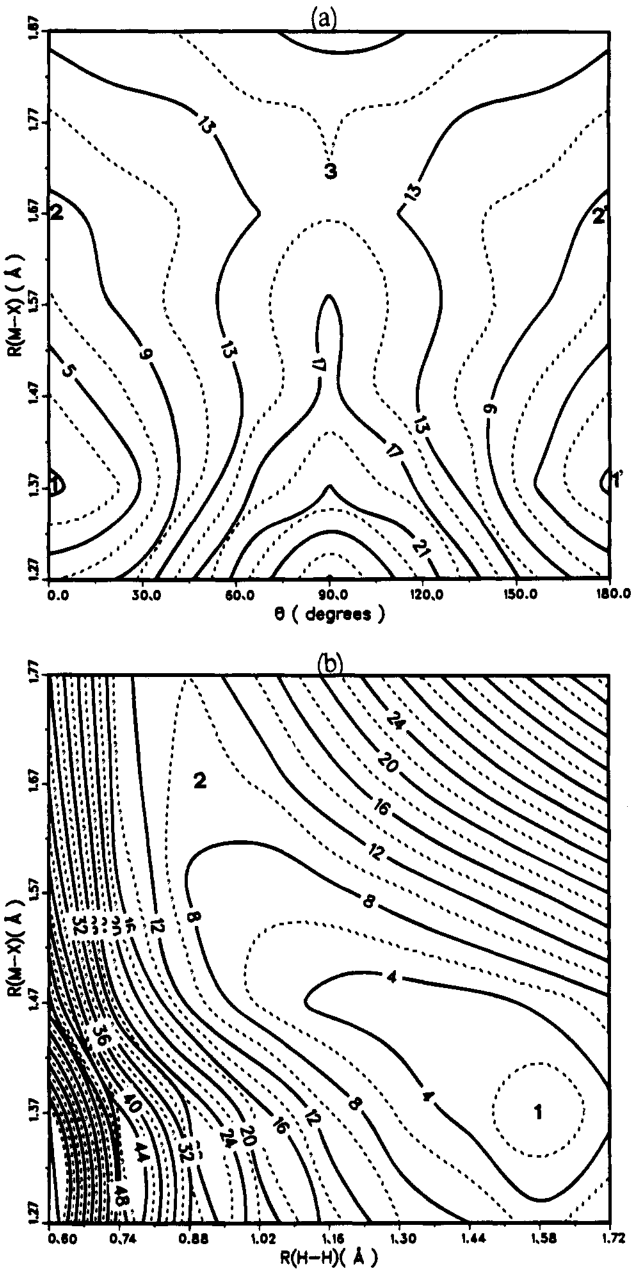

Figure 1. Bidimensional potential reduced energy surfaces for the H−H exchange coupling. Contour energies are in kcal/mol. (a) The surface is obtained by optimizing the $R_{HH}$ distance for each pair of $R_{MX}$ and $\theta$ parameters in the 3-D surface (see Scheme 2). (b) Cut of the 3-D surface at $\theta = 0°$.

**Table 2.** MP2 Transition State Geometry for the Exchange Coupling in the $[(C_5H_5)Ir(PH_3)H_3]^+$ Complex[a]

| | | | | | |
|---|---|---|---|---|---|
| Ir−$H_1$ | 1.745 | $H_1 \cdots H_2$ | 0.892 | ∠$H_1$−Ir−$H_2$ | 29.6 |
| Ir−$H_2$ | 1.745 | $H_1 \cdots H_3$ | 2.432 | ∠$H_1$−Ir−$H_3$ | 93.3 |
| Ir−$H_3$ | 1.597 | $H_2 \cdots H_3$ | 2.084 | ∠$H_2$−Ir−$H_3$ | 77.0 |
| Ir−P | 2.398 | | | ∠$H_1$−Ir−P | 108 |
| Ir−C | 2.376 | | | ∠$H_2$−Ir−P | 83.0 |
| | | | | ∠$H_3$−Ir−P | 85.6 |

[a] Distances are given in Å and angles in deg.

In order to apply the one-dimensional tunneling model we now face the problem of building up the reaction path for the hydrogen exchange process. The more systematic way to do that would require the methodology of the Intrinsic Reaction Coordinate[16] (IRC) where the reaction path starts up at the

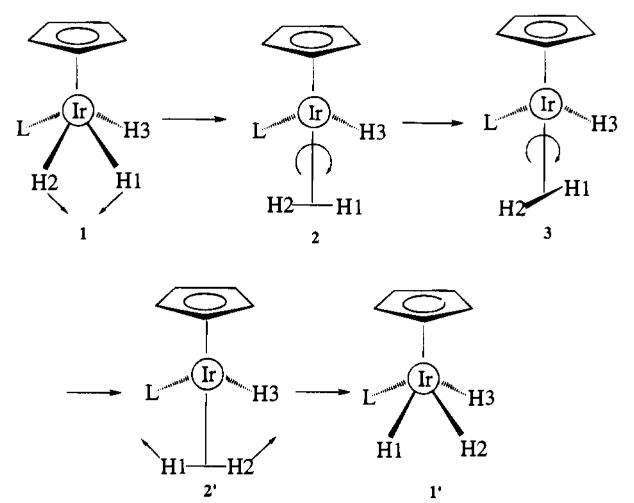

**Figure 2.** Structures obtained for the hydrogen exchange mechanism along the proposed path. Numbers identifying the different structures relate to their position in the potential energy surface (see Figure 1).

transition state by following the eigenvector associated to the negative eigenvalue of the second-derivative energy matrix and then heads on to the minimum energy structure through a steepest descent path in mass-weighted Cartesian coordinates. Due to the size of the system, however, the calculations needed to obtain the complete IRC are well beyond our present computer capabilities.

Given that the direction of the eigenvector which has an imaginary frequency in the transition state clearly indicates a rotation of the two exchanging hydrogens (angle $\theta$), we have chosen as a reaction path the one that begins at the transition state by rotating the two exchanging hydrogens from $\theta = 90°$ up to the planar ($\theta = 0°$) conformation. In this manner point **2** indicated in Figure 1a is reached. This point has a $\eta^2$-$H_2$ structure with $R_{MX} = 1.67$ Å and $R_{HH} = 0.88$ Å. It lies 8.7 kcal/mol above the minimum.[17,18] This structure, however, does not correspond to an actual minimum of the whole surface as a fully MP2 optimization of it leads to the trihydride minimum already located. In this way the path that passes through point **2** is the shortest one (in mass-weighted Cartesian coordinates) that joins points **3** and **1**.

The reaction path we propose can be better envisaged by looking at Figure 2. Starting from point **1**, a lengthening of the Ir−X distance and a shortening of the $H_1$−$H_2$ distance take place, eventually reaching point **2**. Then the $H_1$−$H_2$ rotation from $\theta = 0°$ to 90° occurs in order to reach the transition state (point **3**). From here the motions are reversed, the path passing consecutively through points **2′** and **1′** which are the symmetric counterparts of points **2** and **1**.

To better understand the evolution of the H−H distances along the reaction path in Figure 1b we have located points **1** and **2** which can be joined by a steepest descent path. This corresponds to the planar zone ($\theta = 0°$) of the reaction path. After point **2** has been reached, $\theta$ begins to increase in order to reach point **3** so that the reaction path can no longer be found in the cut of the surface $\theta = 0°$ depicted in Figure 1b.

**Table 3.** MP2 Geometries for the Minimum and the Transition State for the $[(C_5H_5)Ir(CO)H_3]^+$ Complex[a]

| | min | TS | | min | TS |
|---|---|---|---|---|---|
| Ir−$H_1$ | 1.604 | 1.796 | $H_1$−Ir−$H_2$ | 62.8 | 27.6 |
| Ir−$H_2$ | 1.601 | 1.796 | $H_1$−Ir−$H_3$ | 62.8 | 92.1 |
| Ir−$H_3$ | 1.601 | 1.600 | $H_2$−Ir−$H_3$ | 117.0 | 78.3 |
| Ir−$C_{C=O}$ | 2.007 | 2.011 | $H_1$−Ir−$C_{C=O}$ | 103.0 | 108.3 |
| Ir−$C_{Cp}$ | 2.386 | 2.378 | $H_2$−Ir−$C_{C=O}$ | 81.9 | 83.6 |
| $H_1$−$H_2$ | 1.671 | 0.857 | $H_3$−Ir−$C_{C=O}$ | 81.9 | 86.5 |
| $H_1$−$H_3$ | 1.671 | 2.449 | | | |
| $H_2$−$H_3$ | 2.737 | 2.150 | | | |

[a] Distances are given in Å and angles in deg.

A mechanism related to the one proposed here has been described by Limbach *et al.*[19] That mechanism occurs in two steps: first, a metastable dihydrogen complex is formed by an activated rate process; subsequently, rotational tunneling takes place. The mechanism we propose differs from Limbach's mechanism in that our MP2 calculations show that a minimum energy structure corresponding to a metastable dihydrogen complex does not exist. In addition, our description of the reaction path clearly indicates that the process actually involves a vibrational tunneling mechanism.

Once the reaction path has been clearly defined, the tunneling model described in the methodology section can be readily applied. The energy barrier of the double well is that obtained for the transition state located in the full-dimensional MP2 potential energy surface. The path length has been evaluated by geometrical analysis of the reaction path obtained in the three-dimensional reduced surface. In this manner we have calculated an exchange coupling $-2J$ of 112.3 Hz, a result which compares very well with the total observed coupling measured at the lower ($T = 176$ K) temperature for the similar $[(C_5H_5)Ir(PMe_3)H_3]^+$ complex (96 Hz).[1b]

## IV. Effect of Ligand Substitution

The effect of the ligands in the exchange coupling of $[(C_5H_5)Ir(L)H_3]^+$ complexes has been extensively studied by Heinekey *et al.*[1b] Experimental results show that the coupling increases when the $\pi$-acceptor character of the ligand L is enhanced. To study the effect of the ligand substitution on the quantum exchange process we have chosen to substitute the $PH_3$ group by a carbonyl CO group. As is well-known, CO is a good $\pi$-acceptor group so that it tends to diminish the electronic density at the iridium atom, and so the $\pi$ back-donation to the $\sigma^*$ orbital of $H_2$ diminishes. As a consequence, it is to be expected that the presence of the CO group will make more favorable the appearance of $\eta^2$-$H_2$ configurations than for the $PH_3$ group. Given that both points **2** and **3** on the potential energy surface (Figure 1a) have a $\eta^2$-$H_2$ configuration, the energy barrier should be lower in this case, noticeably increasing the exchange coupling.

According to this analysis we have considered next the $[(C_5H_5)Ir(CO)H_3]^+$ complex for which calculations very similar to the ones described in the preceding section have been carried out. Results can be summarized in the geometries of the MP2 fully optimized minimum energy structure and transition state shown in Table 3. Results in this table clearly show that the minimum energy structure again has a trihydride structure and the transition state contains a 90° rotated dihydrogen entity. Rotation of the dihydrogen in the transition state leads to a $\eta^2$-$H_2$ structure which has an energy 6.1 kcal/mol above the trihydride minimum. This structure is analogous to point **2**

---

(16) (a) Fukui, K. *J. Phys. Chem.* **1970**, *74*, 4161. (b) Truhlar, D. G.; Kupperman, A. *J. Am. Chem. Soc.* **1971**, *93*, 1840. (c) Fukui, K. *Acc. Chem. Res.* **1981**, *14*, 3613. (d) Fukui, K. *Int. J. Quantum Chem.* **1981**, *15*, 633. (e) Fukui, K. *Pure Appl. Chem.* **1982**, *54*, 1825.

(17) Hall *et al.*[18] reported that at the MP2 level the trihydride structure is more stable than the $\eta^2$-$H_2$/H for the $[(C_5H_5)Ir(L)H_3]^+$ complexes. The difference in energies is 11.7 kcal/mol for L = $PH_3$ and 8.7 kcal/mol for L = CO. It is not verified, however, whether the $\eta^2$-$H_2$ structures are true minima of the potential energy surfaces.

(18) Lin, Z.; Hall, M. B. *Organometallics* **1992**, *11*, 3801.

(19) Limbach, H. H.; Scherer, G.; Maurer, M.; Chaudret, B. *Angew. Chem., Int. Ed. Engl.* **1992**, *31*, 1369.

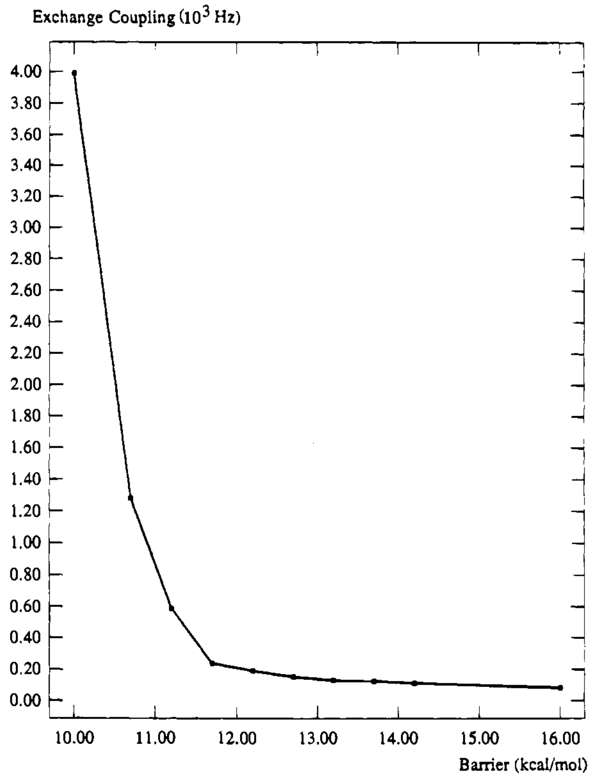

**Figure 3.** Dependence of the exchange coupling on the barrier height.

located in the surface for the L = $PH_3$ complex (see Figure 1a). Again, this point is not a minimum at the MP2 level as a full geometry optimization leads to the trihydride minimum.[17,18]

The energy barrier imposed by the transition state is 10.7 kcal/mol, which has to be compared with the value of 14.1 kcal/mol for the $PH_3$ case. This lower energy barrier leads to a clearly higher exchange coupling $-2J$ of 1279.5 Hz. This result confirms the above-mentioned expectations for the CO complex. Analysis of the NMR spectra for this complex also indicates an important increment of the exchange coupling for the carbonyl compound.[20,21]

At this point it should be emphasized that the exchange coupling is proportional to the tunneling rate. In this way, the dependence on the energy barrier is roughly exponential. As a consequence, exchange coupling is very sensitive to the precision with which the energy barrier can be determined. A small, acceptable error (for instance 1 or 2 kcal/mol) in the theoretical energy barrier can cause an important deviation in the predicted value of $-2J$. So, the theoretical $-2J$ values obtained in this work should be taken as an approximation that determines their order of magnitude. In this sense the difference of the $-2J$ values found between the $[(C_5H_5)Ir(PH_3)H_3]^+$ and $[(C_5H_5)Ir(CO)H_3]^+$ complexes is significant enough to show a clear distinct behavior of the $PH_3$ and CO ligands, which reflects the experimental findings.

In order to understand the dependence of the exchange coupling on the barrier height we have used our one-dimensional tunneling model to compute $-2J$ for a variety of energy barrier values, the path length used being the one corresponding to the $[(C_5H_5)Ir(PH_3)H_3]^+$ complex (roughly the same value as that associated with the $[(C_5H_5)Ir(CO)H_3]^+$ complex). So, Figure 3 shows how extremely sensitive exchange coupling is to the barrier height, specially below 11–12 kcal/mol, where $-2J$ increases very sharply. This explains why a slight change of the electronic properties of the ligands noticeably modifies the experimentally observed couplings. Conversely, when the barrier increases the exchange coupling slowly decreases, so that at the limit of infinite barrier the exchange coupling will vanish.

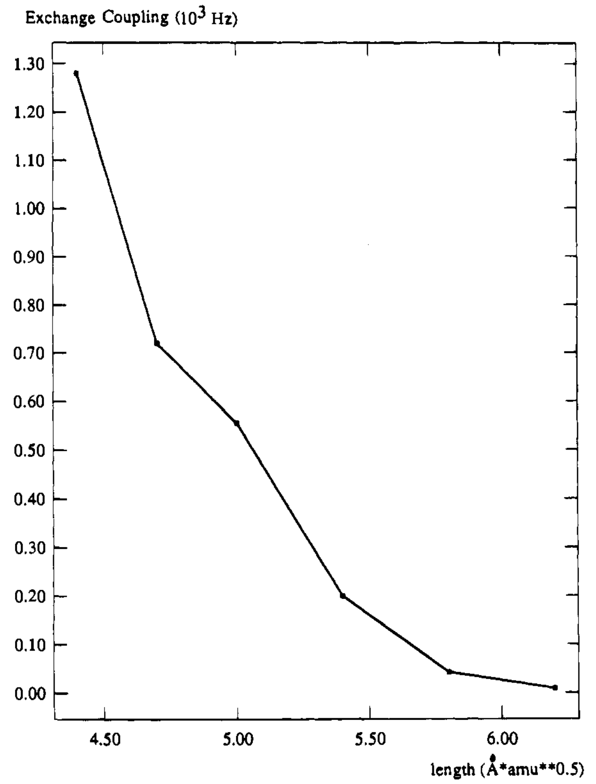

**Figure 4.** Dependence of the exchange coupling on the total path length (in mass-weighted Cartesian coordinates).

A point that can also been discussed now is whether the MP2 level of calculation is enough to obtain reliable couplings. A previous calculation (ref 13c) suggests that at the higher MP4 level results may differ considerably from the MP2 results. In order to test this point we have calculated the energy at the MP4 level (including simple, double, triple, and quadruple excitations) for the transition state and the minimum energy geometries as obtained at the MP2 level for both L = $PH_3$ and CO cases. As indicated by the results of Maseras et al.,[13c] the MP4 barriers are lower: 11.6 and 8.1 kcal/mol for L = $PH_3$ and CO, respectively. Figure 3 indicates that this lowering of the barrier will not considerably affect the L = $PH_3$ case whereas a clear high coupling will come out for the L = CO case. This last result would be in closer agreement with experimental results.[20] Therefore, the main qualitative predictions of this paper are not modified by differences of 2–3 kcal/mol in the energy barriers in spite of the roughly exponential dependence of the exchange coupling on the barrier.

Another interesting point to be tested is the dependence of the exchange coupling on the path length. To this end, we have employed the one-dimensional tunneling model to calculate $-2J$ within a range of path length values. We have taken the energy barrier for the $[(C_5H_5)Ir(CO)H_3]^+$ complex. The results are displayed in Figure 4, where it is evident that exchange coupling rapidly decreases as the path length increases. The point at 4.40 amu$^{1/2}$·Å corresponds to the $[(C_5H_5)Ir(CO)H_3]^+$ complex, whereas the point at 6.75 amu$^{1/2}$·Å arises from the $[(C_5H_5)Ir(CO)D_2H]^+$ isotopomer complex in which a pair of deuteriums are exchanging. We will come back later to this isotope effect.

---

[20] The NMR spectrum of the complex with L = CO indicates that, in this case, the total observed coupling could be bigger than 20000 Hz.[21]

[21] Heinekey, D. M. Personal Communication.

**Table 4.** Lowest Three Vibrational Pairs of Levels for the $[(C_5H_5)Ir(PH_3)H_3]^+$ Exchange Coupling Process

| $n$ | $E_{rel}$ (kcal/mol) | $-2J$ (Hz) |
|---|---|---|
| 1 | 0 | 112.3 |
| 2 | 2.57 | 290.7 |
| 3 | 6.94 | 10491.1 |

**Table 5.** Occupancy of the Three Lowest Pairs of Vibrational Levels ($P_i$) and Total Exchange Coupling at Different Temperatures for the $[(C_5H_5)Ir(PH_3)H_3]^+$ Complex

| $T$ (K) | $P_1$ | $P_2$ | $P_3$ | $-2J$ (Hz) |
|---|---|---|---|---|
| 50 | 1.00 | $6.06 \times 10^{-12}$ | $5.11 \times 10^{-31}$ | 112.3 |
| 100 | 1.00 | $2.46 \times 10^{-6}$ | $7.15 \times 10^{-16}$ | 112.3 |
| 150 | 1.00 | $1.82 \times 10^{-4}$ | $7.99 \times 10^{-11}$ | 112.3 |
| 200 | 1.00 | $1.57 \times 10^{-3}$ | $2.67 \times 10^{-8}$ | 112.6 |
| 250 | 0.99 | $5.68 \times 10^{-3}$ | $8.69 \times 10^{-7}$ | 113.4 |
| 300 | 0.99 | $1.33 \times 10^{-2}$ | $8.82 \times 10^{-6}$ | 117.1 |
| 330 | 0.98 | $1.96 \times 10^{-2}$ | $2.52 \times 10^{-5}$ | 128.6 |
| 350 | 0.98 | $2.44 \times 10^{-2}$ | $4.59 \times 10^{-5}$ | 149.9 |
| 370 | 0.97 | $2.96 \times 10^{-2}$ | $7.82 \times 10^{-5}$ | 195.8 |
| 390 | 0.96 | $3.52 \times 10^{-2}$ | $1.26 \times 10^{-4}$ | 287.2 |
| 400 | 0.96 | $3.81 \times 10^{-2}$ | $1.57 \times 10^{-4}$ | 359.6 |

## V. Temperature Dependence

A pronounced temperature dependence has been experimentally observed for the couplings of transition-metal trihydride complexes.[1-4] For instance, the observed coupling varies from 96 to 135 Hz between 176 and 196 K for the $[(C_5H_5)Ir(PMe_3)H_3]^+$ complex.[1b] Our theoretical methodology should be able to reproduce this experimental trend. Up to this point we have only dealt with quantum exchange in the ground pair of vibrational states. To take into account the temperature effect, higher lying pairs of vibrational states have to be considered as well. The results for the $[(C_5H_5)Ir(PH_3)H_3]^+$ complex are presented in Tables 4 and 5. In Table 4 $n$ stands for the ordering of each pair of near degenerate vibrational states (only the first three are shown), while $E_{rel}$ is the average energy of each pair relative to the ground pair. Since the vibrational pairs are widely spaced, it will be assumed that the exchange process can be considered separately in each pair.

As expected, one can see that at higher energies of the pair, the splitting increases very fast. At low temperatures only the ground pair is significantly occupied (see Table 5), leading to an exchange coupling of 112.3 Hz. As the temperature increases the higher pairs become slightly populated. Because the transition rate from one vibrational state to another is expected to be very fast, the exchange coupling turns out to be a population weighted average according a Boltzman distribution over the thermally accessible pairs of vibrational states. The influence of the second vibrational pair begins at 200 K, while the sharp increase of the averaged exchange coupling is essentially due to the contribution of the third and higher lying vibrational pairs. An analogous behavior has been found for the $[(C_5H_5)Ir(CO)H_3]^+$ complex. In this way the temperature dependence of the exchange coupling for the $[(C_5H_5)Ir(PH_3)H_3]^+$ and $[(C_5H_5)Ir(CO)H_3]^+$ complexes has been depicted in Figure 5, showing a large increase after the vibrational pairs above the ground pair begin to be significantly populated, so that the experimental trend is reproduced. Perhaps the one drawback of this model is that the theoretical curves are quite flat up to higher temperatures as compared with the experimental case. This is likely an artifact of the one-dimensional tunneling model which exaggerates the energy difference between the excited vibrational pairs. Tunneling models of higher dimensionality would probably be required to eliminate this problem.

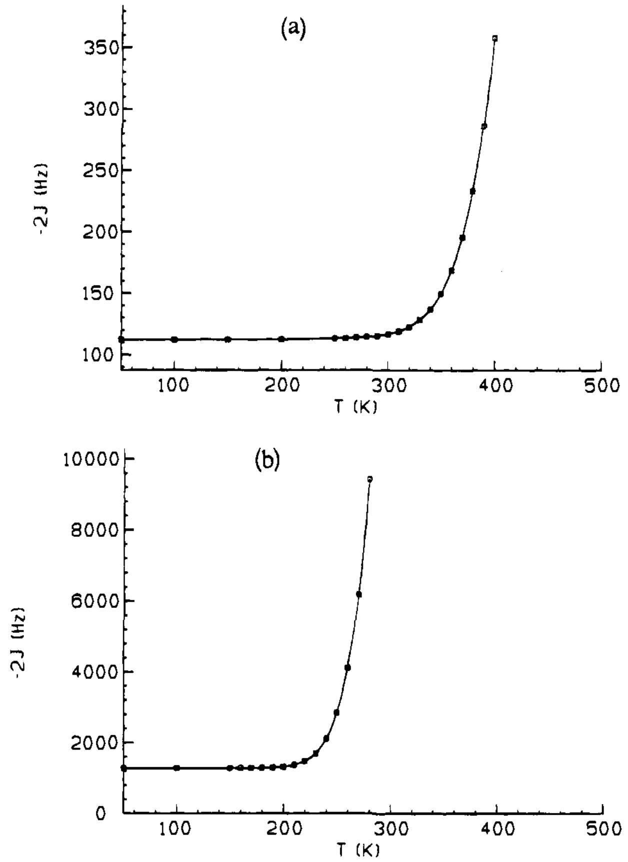

**Figure 5.** Temperature dependence of the exchange coupling $-2J$ for the $[(C_5H_5)Ir(L)H_3]^+$ complexes: (a) L = $PH_3$. (b) L = CO.

**Scheme 3**

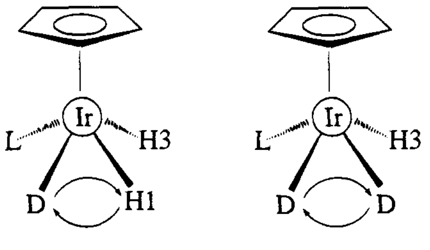

a b

## VI. Isotope Effects

A convincing positive proof that the large observed $^1H^1H$ couplings on the transition metal trihydrides are not magnetic in origin lies in the experimental absence of any resolvable $^1H^2D$ coupling and the very small $^1H^3T$ couplings observed in partially deuterated or tritiated isotopomers, respectively.[1b]

These results suggest again the existence of a quantum mechanical exchange that can be quenched by the excess of mass derived from the isotopic substitution. To theoretically study this phenomenon, in this section we will be concerned with the primary isotope effect that appears when one or both exchanging $^1H$ are replaced by deuteriums. To this end we have calculated the exchange coupling for the complexes presented in Scheme 3. The corresponding one-dimensional double wells for the case L = $PH_3$, along with the one associated with the perprotio species, have been represented in Figure 6. Note that, according to the Born–Oppenheimer approximation, the electronic energy and, as a consequence, the energy barriers without zero-point correction are not dependent on the isotopic substitution. Conversely, in mass-weighted Cartesian coordinates, the

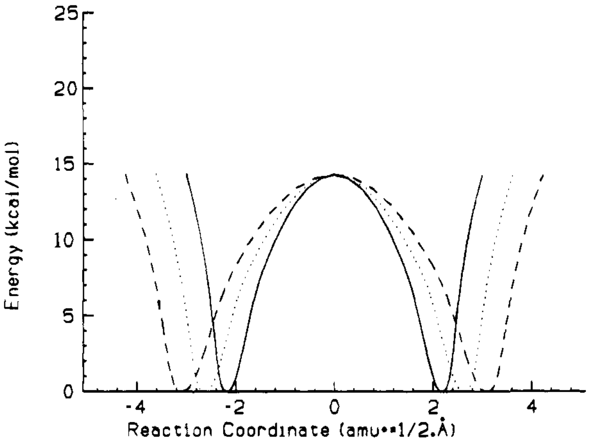

**Figure 6.** Effect of the isotopic substitution on the total path length for the exchange coupling process. Solid line: both exchanging particles are $^1H$. Dotted line: The exchanging particles are $^1H$ and $^2D$. Dashed line: Both exchanging particles are $^2D$.

path length is enhanced as the number of $^1H$ substituted by deuterium increases.[22] This fact leads directly to the quenching of the tunneling and, therefore, to a very drastic diminution of the exchange tunneling for the complexes with two exchanging deuteriums (Scheme 3b). So, we have obtained exchange couplings of only 6.04 and 9.48 Hz for L = $PH_3$ and L = CO, respectively.

The situation is slightly more complicated for the complex of Scheme 3a, containing only one deuterium. In this case the increase of the path length is not the important factor as the particles which are interchanging between inequivalent sites A and B are now not identical (a hydrogen and a deuterium). As a result of the change in vibrational frequencies due to the change in mass, the double well will no longer be energetically degenerate.[22] To take this fact into account we have calculated the vibrational frequencies at both minima. Then, our original double well profile has been asymmetrized so that the energy difference between minima coincides with the difference in zero-point energy. Numerical evaluation of this slightly asymmetric double well confirms the quenching of the quantum exchange coupling as now the vibrational levels become fully located at one side of the double well. This result explains the inability to observe the exchange coupling in the NMR spectra of these asymmetrically substituted isotopes.

## VII. Conclusions

In this paper we have provided theoretical calculations based on first principles that confirm that the very large values of the apparent $J_{AB}$ couplings observed for complexes of the type $[(C_5H_5)Ir(L)H_3]^+$ can be explained by a tunneling exchange mechanism. This produces a coupling $-2J$ that can be added to the magnetic coupling, leading to a total value which can be measured experimentally in the NMR spectra.

Given that this exchange coupling is very sensitive to the precision with which the energy barrier is calculated, we can only expect agreement in the order of magnitude with the measured coupling. Anyway it has to be noted that we are comparing the theoretical exchange coupling with the total observed coupling which includes a contribution of 25−30 Hz coming from the magnetic scalar coupling. However, our methodology is good enough to correctly predict the effect of ligand substitution, the temperature dependence, and the effect of isotopic substitution on the exchange coupling value.

Although this phenomenon has been observed first in some trihydride complexes, it has to be expected that it can be present in a wider range of compounds. The only required condition is that the energy barrier is low enough and the reaction path length is short enough so that the exchange coupling of a pair of hydrogens has a non-negligible value. As a matter of fact, the procedure by which the energy splitting appears in the radiofrequency zone of the spectrum is not essentially different than other previously studied phenomena. A well-known example is the rotational tunneling of dihydrogen transition metal complexes[23] that is known to have an energy splitting in the microwave range of the electromagnetic spectra.

**Acknowledgment.** Financial support for this work was provided by the Dirección General de Investigación Científica y Técnica DGICYT through projects PB92-0613 and PB92-0621. Computational facilities by the Centre de Supercomputació de Catalunya, CESCA and the Center of Parallelism of Barcelona, CEPBA are also acknowledged.

JA940984Q

---

(22) Bosch, E.; Moreno, M.; Lluch, J. M. *J. Am. Chem. Soc.* **1992**, *114*, 4832.

(23) (a) Eckert, J.; Kubas, G. J.; Dianoux, A. J. *J. Chem. Phys.* **1988**, *88*, 466. (b) Eckert, J.; Kubas, G. J.; Hall, J. H.; Hay, P. J.; Boyle, M. B. *J. Am. Chem. Soc.* **1990**, *112*, 2324. (c) Eckert, J.; Jensen, C. M.; Jones, G.; Clot, E.; Eisenstein, O. *J. Am. Chem. Soc.* **1993**, *115*, 11056.